

Synthesis and structure characteristics of the new ternary boride $(V_{1-x}Nb_x)_2B_3$

Yang Yu, Torsten Lundström

Institute of Chemistry, Uppsala University, Box 531, S-751 21 Uppsala, Sweden

Received 8 May 1995

Abstract

The new ternary compound $(V_{1-x}Nb_x)_2B_3$ was synthesized by both single crystal and polycrystalline methods. It belongs to the V_2B_3 -type structure, which crystallizes in the orthorhombic space group $Cmcm$ (No. 63), with $Z = 4$. The unit cell parameters of the ternary compound vary in the ranges 3.1086–3.162 Å, 18.5817–19.107 Å and 3.0114–3.086 Å for a , b and c respectively, with the V/Nb ratios in the starting materials varied from 3 to 1/2. The crystal structure of one representative single crystal of $(V_{1-x}Nb_x)_2B_3$ was studied by single crystal X-ray diffractometry. The structure refinement converged at an $R(F^2)$ value of 0.042 for 1165 reflections. For the single crystal studied, the composition calculated from the refinement was $(V_{0.82}Nb_{0.18})_2B_3$. In the crystal structure of $(V_{0.82}Nb_{0.18})_2B_3$, 73.9% of the niobium atoms occupy the V(1) position, while the remaining atoms occupy the V(2) position. The influence of the V/Nb ratio in the starting materials on the formation of the $(V_{1-x}Nb_x)_2B_3$ compound and the unit cell parameters is discussed.

Keywords: Vanadium niobium boride; Ternary boride; Crystal structure; Synthesis

1. Introduction

Synthesis and crystal structure of the prototype binary boride V_2B_3 have been studied by both powder and single crystal methods [1,2]. In addition, two further binary representatives of V_2B_3 have been reported [3,4]. Up to now, two ternary representatives of the V_2B_3 -type structure have been reported, namely Cr_3NiB_6 [5] and $CoVB_3$ [6]. For the latter, a single crystal X-ray diffraction study was performed by the film technique and an order of the metal atoms was found [6].

In the present work, single crystal growth and polycrystalline sample preparations of the ternary $(V_{1-x}Nb_x)_2B_3$ were carried out. The order of the metal atoms in $(V_{1-x}Nb_x)_2B_3$ was studied by a single crystal structure refinement.

2. Experimental details

2.1. Synthesis of $(V_{1-x}Nb_x)_2B_3$

The synthesis of polycrystalline samples of $(V_{1-x}Nb_x)_2B_3$ was performed by arc-melting the start-

ing materials followed by heat treatment. The claimed purities of the starting materials were 99.6% (H.C. Starck, Goslar, Germany), 99.95% (Materials Research, Toulouse, France) and 99.4% (H.C. Starck, Goslar, Germany) for crystalline boron, vanadium lumps and niobium powder respectively. The crystalline boron was crushed into fine powder and the vanadium metal lumps were cut into small pieces. The mixtures of the starting materials were pressed into pellets and then arc-melted under an argon atmosphere (AGA, Sundbyberg, Sweden, claimed purity 99.9998%). The solidified samples were subsequently heat treated in a resistance furnace at 1300°C for 24 h under an argon atmosphere (claimed purity 99.998%).

Single crystal growth of ternary $(V_{1-x}Nb_x)_2B_3$ was performed by the high temperature metal solution method using aluminium flux [7,8]. The claimed purity for aluminium metal was 99.997% (Vigeland's Bruk, Norway). The synthesis was performed in a vertical graphite furnace (Thermal Technology Inc. 1000-3560-FP-20) under a flow of pure argon gas. The mixture of the starting materials was placed in an alumina crucible and initially heated to 1650°C, soaked at this temperature for 5 h, then cooled to 1000°C at a cooling rate of 50°C h⁻¹ whereafter the furnace was

switched off. The as-grown crystals were separated from the solidified excess aluminium in diluted hydrochloric acid (6 M). Preparation data for both polycrystalline and single crystal samples are listed in Table 1.

2.2. X-ray and element analysis

X-ray powder diffraction patterns were recorded using a Guinier–Hägg camera with strictly monochromatic Cu $K\alpha_1$ radiation ($\lambda = 1.540598 \text{ \AA}$) and semiconductor-grade silicon ($a = 5.431065 \text{ \AA}$) as internal calibration standard [9]. The unit cell parameters were determined by least-squares refinement using the local program UNITCELL [10]. The unit cell dimensions of each $(V_{1-x}Nb_x)_2B_3$ sample corresponding to different initial proportions of the starting materials are listed in Table 1. Electron microprobe analyses of the $(V_{1-x}Nb_x)_2B_3$ crystals were performed in an SEM (JEOL JSM-840) equipped with an energy dispersive detector. The aluminium concentration was found to be below the limit of detection for the above-mentioned crystals. A semi-quantitative element analysis was made on the surface of the as-grown single crystals from different batches. Since boron is a light element, its concentration could only be obtained by difference using this method. The measured Nb/V ratios for these crystals were in the range of 0.02–0.61. A well-formed single crystal of $(V_{1-x}Nb_x)_2B_3$ with suitable size was selected for X-ray intensity measurement.

2.3. Intensity measurement and crystal structure refinement

Details of crystal data, X-ray intensity data collection and refinement parameters are listed in Table 2. The collected intensity data were corrected for Lorentz-polarization, decay and absorption effects. Absorption corrections were applied using the Gaussian grid technique. All these pre-refinement corrections of the original reflection data were carried out using the TEXSAN software system [11].

The structure refinement of $(V_{1-x}Nb_x)_2B_3$ was car-

Table 2
Crystal data, data collection and refinement parameters

Crystal data	
Formula	$(V_{0.82}Nb_{0.18})_2B_3$
Formula weight	149.42
Space Group, Z	<i>Cmcm</i> , 4
Cell parameters (\AA)	$a = 3.1086(5)$ $b = 18.5817(9)$ $c = 3.0114(4)$
Cell volume (\AA^3)	$V = 174.0$
Crystal dimensions (mm)	$0.1 \times 0.08 \times 0.08$
No. of boundary planes	8
D_{calc} (g cm^{-3})	5.69
Absorption coefficient (cm^{-1})	102.48
Data collection	
Diffractometer	Rigaku AFC6R
Radiation, λ (\AA)	Mo, $K\alpha$, 0.71069
$2\theta_{min}$, $2\theta_{max}$	124.6°
Scan type	ω - 2θ
Scan width (deg)	$1.31 = 0.35\text{tg}\theta$
scan speed (deg min^{-1})	8
h, k, l	(-1,8), (-11,46), (-1,8)
No. of standard reflections	6
Standard interval (ref.)	150
Decay (%)	1.1
Transmission	0.61–0.66
Reflections:	
measured	1165
observed ($>3\sigma$)	836
independent	818
Refinement	
Weighting scheme	$w^{-1} = (1.35\sigma)^2 + (0.006Y_0)^2$
S	1.15
No. of parameters refined	24
No. of parameters constrained	10
$R(F^2)$	0.042
$R_w(F^2)$	0.051

ried out using the full-matrix least-squares program DUPALS [12]. The initial values for the atomic coordinates and displacement factors were taken from Ref. [2]. Since there are two different atomic positions for the metal atoms in the V_2B_3 -type crystal structure, the niobium atoms may be distributed according to three different schemes, namely at the V(1) or V(2) sites or at both sites. All three possible situations were tested in the crystal structure refinements. For each situation,

Table 1
Sample preparation data and unit cell dimensions of $(V_{1-x}Nb_x)_2B_3$

	Polycrystalline samples					Single crystal samples		
	3	2	1	1/2	1/3	3	2	1
V/Nb	3	2	1	1/2	1/3	3	2	1
B/(V + Nb)	3/2	3/2	3/2	3/2	3/2	3/2	1.45	1.45
Al/(V + Nb)	—	—	—	—	—	28	28	28
a (\AA)	3.1449(5)	3.1564(5)	3.159(1)	3.162(2)	—	3.1181(5)	3.1417(5)	3.1578(4)
b (\AA)	18.689(2)	18.773(2)	18.966(9)	19.107(8)	—	18.610(4)	18.670(4)	18.730(4)
c (\AA)	3.0216(4)	3.0347(4)	3.058(2)	3.086(2)	—	3.0104(4)	3.0219(4)	3.0312(3)
V (\AA^3)	177.6	179.8	183.2	186.4	—	174.7	177.3	179.3

Table 3

Final structure data for $(V_{0.82}Nb_{0.18})_2B_3$, where the estimated standard deviations are given in parentheses^a

Atom	Position	x	y	z	Occupancy	$B_{(eq)}$ (\AA^2)	U_{11}	U_{22}	U_{33}
V(1)	4c	0	0.42909(2)	0.25	0.74(1)	0.32(1)	47(1)	33(1)	40(1)
Nb(1)	4c	0	0.42907(2)	0.25	0.26(1)	0.28(1)	42(1)	27(1)	35(1)
V(2)	4c	0	-0.29495(2)	0.25	0.91(1)	0.31(1)	47(1)	31(1)	38(1)
Nb(2)	4c	0	-0.29498(2)	0.25	0.09(1)	0.22(1)	38(1)	18(1)	29(1)
B(1)	4c	0	0.0235(1)	0.25	1	0.36(7)	70(10)	20(10)	40(10)
B(2)	4c	0	0.1184(1)	0.25	1	0.34(7)	60(10)	30(10)	40(10)
B(3)	4c	0	-0.1694(1)	0.25	1	0.31(7)	60(10)	30(10)	30(10)

^a The displacement factor is described as $\exp\{-2\pi^2(U_{11}h^2a^{*2} + U_{22}k^2b^{*2} + U_{33}l^2c^{*2} + 2U_{12}hka^*b^* + 2U_{13}hla^*c^* + 2U_{23}klb^*c^*)\}$, where $U_{12} = U_{13} = U_{23} = 0$. $R = 0.042$, $R_w = 0.051$, for all measured reflections U_{11} are given in $\text{\AA}^2 \times 10^4$.

the positional parameters, isotropic displacement parameters and the occupancy factor for niobium atoms were constrained to the corresponding parameters of the vanadium atom(s). The refinement showed that most of the niobium atoms occupy the V(1) sites, although they were found at both V(1) and V(2) atomic positions. A systematic extinction effect was found and consequently an extinction correction (type I isotropic extinction) was applied in the refinement. The anisotropic displacement parameters were then refined for the vanadium and boron atoms and constrained for the niobium atom. Prior to the final refinement, all the structure parameters were fixed except the positional and anisotropic displacement parameters of the niobium atom. No significant difference was found for the positional parameter between the vanadium and niobium atoms. For the anisotropic displacement parameters, however, differences were found between the vanadium and niobium atoms. The final structure data are presented in Table 3 and the interatomic distances in Table 4.

Table 4

Interatomic distances in $(V_{0.82}Nb_{0.18})_2B_3$ ^a

Atoms	Distance (\AA)	Atoms	Distance (\AA)
TM(1)–2TM(1)	3.0114(7)	B(1)–2B(1)	1.741(2)
–2TM(1)	3.0350(8)	–2B(1)	3.0114(7)
–2TM(1)	3.1086(8)	–2B(1)	3.1086(8)
–2TM(2)	2.9120(7)	–2B(2)	3.036(3)
–4B(1)	2.336(1)	–2B(3)	3.100(3)
–2B(1)	2.344(2)		
–4B(2)	2.337(1)	B(2)–2B(2)	3.0114(7)
–2B(3)	2.401(2)	–2B(2)	3.1086(8)
		–2B(3)	1.779(2)
TM(2)–4TM(2)	2.7339(6)		
–2TM(2)	3.0114(7)	B(3)–2B(3)	3.0114(7)
–2TM(2)	3.1086(8)	–2B(3)	3.1086(8)
–2B(2)	2.238(2)		
–4B(3)	2.2634(8)		
–B(3)	2.334(2)		

^a Since vanadium and niobium atoms are at the same atomic positions, both of them are expressed as TM. Distances listed are all TM–TM < 3.6 \AA and B–B < 3.2 \AA . The estimated standard deviations are given in parentheses.

3. Results and discussion

3.1. Structure characteristics of $(V_{1-x}Nb_x)_2B_3$

The crystal structure of V_2B_3 (prototype of $(V_{1-x}Nb_x)_2B_3$) has been described in detail in Ref. [2]. As shown in Fig. 1, the TM atoms (TM = V and Nb) occupy two different atomic positions in the crystal structure of $(V_{1-x}Nb_x)_2B_3$. Since these two atomic positions are both at 4c (space group $Cmcm$), they are denoted V(1) and V(2). The TM atoms above and below the boron triple chains are situated in the V(1) positions. The other TM atoms, which are in direct contact and form rectangular pyramids between each slab, are situated in the V(2) positions (see Fig. 1).

In the crystal structure of $(V_{0.82}Nb_{0.18})_2B_3$, the TM

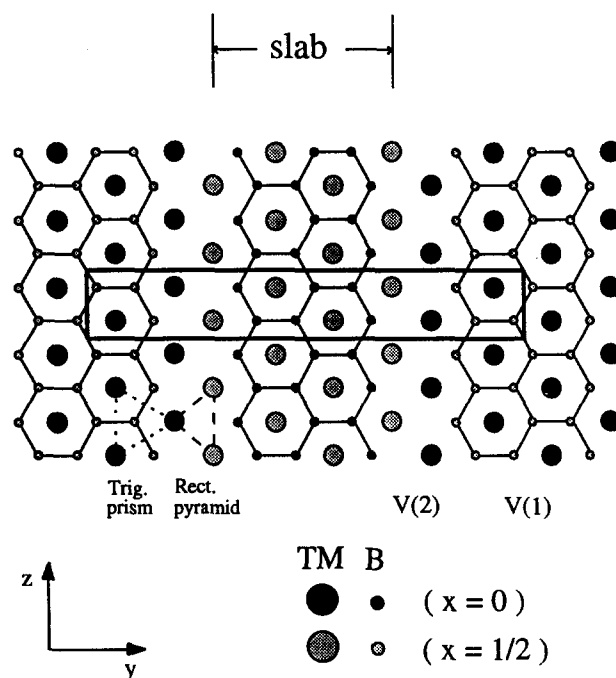


Fig. 1. The crystal structure of $(V_{0.82}Nb_{0.18})_2B_3$ projected in the x -axis direction. The projections of the unit cell, the slab, the trigonal prism, the rectangular pyramid along the same direction, and the atomic positions of V(1) and V(2) are indicated.

atoms are accommodated at the two metal positions with different atomic ratios. In the V(1) position there are 26.9% niobium atoms and in the V(2) positions there are 9.2% niobium atoms (see Table 3), the remaining atoms, of course, being vanadium. This partial order of the metal atoms can also be expressed by saying that 73.9% of the niobium atoms are situated at the V(1) position while 26.1% are at the V(2) position. Thus the larger atom, niobium, prefers the V(1) position, which is at some variance with an earlier hypothesis [2]. From a comparison of the interatomic distances to the atoms surrounding the V(1) and V(2) positions, it can be understood that the larger atom prefers the V(1) position. In $(V_{0.82}Nb_{0.18})_2B_3$, V(1) is surrounded by eight metal neighbours at distances from 2.91 to 3.10 Å and 12 boron atoms at distances from 2.336 to 2.401 Å; V(2) is surrounded by ten metal neighbours at distances from 2.73 to 3.10 Å and seven boron atoms at distances from 2.238 to 2.263 Å (see Table 4). The larger atom thus prefers the position where the nearest atom is at a larger distance, i.e. the energy demand to replace a vanadium atom with a niobium atom is smaller at V(1) than at V(2). The difference must, however, be relatively small, since some niobium also occurs at position V(2).

3.2. Formation of $(V_{1-x}Nb_x)_2B_3$

The ternary phase $(V_{1-x}Nb_x)_2B_3$ was obtained in the samples prepared by both the polycrystalline (arc-melting and heat treatment) and the single crystal method. In addition to $(V_{1-x}Nb_x)_2B_3$, NbAl₃ was found together with the diboride and monoboride in all samples obtained from single crystal growth. As some niobium reacted with the aluminium flux and formed NbAl₃, the B/TM ratio in the flux, which was effective in the formation of the TM borides, increased. Therefore, a decrease of the B/TM ratio (from 3/2 to 1.45) was made in the starting materials as shown in Table 1. However, since single crystals of $(V_{1-x}Nb_x)_2B_3$ were always obtained together with other V–Nb–B phases, the V/Nb ratios in the crystals were not the same as those in the starting materials.

In the polycrystalline samples, no single-phase sample of $(V_{1-x}Nb_x)_2B_3$ was obtained. The ternary phase $(V_{1-x}Nb_x)_2B_3$ invariably crystallized together with the diboride and monoboride when the initial V/Nb ratios were varied from 1/2 to 3. In the sample with V/Nb ratio equal to 1/3, no ternary $(V_{1-x}Nb_x)_2B_3$ was obtained, as shown in Table 1. It was observed during the X-ray analysis that as the V/Nb ratio decreased, the relative intensity of the strongest reflection of the ternary $(V_{1-x}Nb_x)_2B_3$ decreases and the reflections of this phase become broadened. This indicates that on

increasing the nominal niobium content, the relative amount of the ternary $(V_{1-x}Nb_x)_2B_3$ decreases in the phase mixture (sample) and a larger homogeneity range occurs for the ternary $(V_{1-x}Nb_x)_2B_3$. This is in accordance with the experimental result reported by Bolmgren and Lundström [13], who did not obtain any Nb₂B₃ by the polycrystalline (arc-melting and heat treatment) method in the binary Nb–B system.

It is interesting to compare the unit cell volume of the ternary $(V_{1-x}Nb_x)_2B_3$ in samples prepared by both methods. For the same nominal V/Nb ratio, the unit cell volumes of the ternary $(V_{1-x}Nb_x)_2B_3$ prepared by the single crystal growth method are systematically smaller than those prepared by arc-melting and heat treatment, as shown in Table 1. This can be explained by the fact that during single crystal growth of the ternary phase, some of the niobium atoms reacted with the aluminium flux resulting in an increase in the effective V/Nb ratio of the flux, which has the same effect as increasing the nominal V/Nb ratio in the polycrystalline samples.

The unit cell dimensions vs. the atomic ratio of V/Nb of the starting materials of the polycrystalline samples are plotted in Fig. 2. Since the ternary $(V_{1-x}Nb_x)_2B_3$ was never obtained as a single phase in the samples, there is no reason to suppose that the V/Nb ratios of the ternary phase in the samples are the same as the those in the starting materials. It is clearly shown in Fig. 2, however, that all unit cell parameters increase nearly linearly with increasing niobium concentration. The *b* axis expands much more than *a* and *c* with increasing niobium content. It can be seen from Fig. 2 that the slope of the *b* axis vs. V/Nb ratio is nearly constant when the ratio varies from 0.5 to 3.0. As a consequence, it is not possible to draw any conclusion about the order of the niobium atoms in the crystal structure of the ternary $(V_{1-x}Nb_x)_2B_3$ based on the results of phase analysis of the polycrystalline samples.

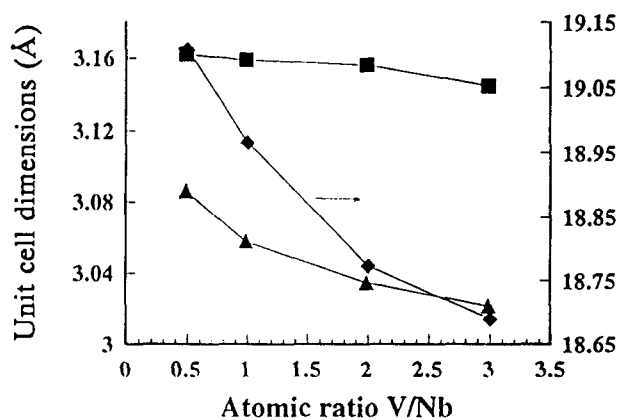


Fig. 2. Unit cell dimensions for $(V_{1-x}Nb_x)_2B_3$ vs. the weighed-in atomic ratios for polycrystalline samples: a, ■; b, ◆; c, ▲.

Acknowledgements

Financial support provided by the Swedish Natural Science Research Council is gratefully acknowledged. The authors are also indebted to Res. Eng. Lars-Erik Tergenius and Anders Lund for their assistance during the experiments.

References

- [1] K.E. Spear and P.W. Gilles, *High Temp. Sci.*, **1** (1969) 86.
- [2] Y. Yu, L.-E. Tergenius, T. Lundström and S. Okada, *J. Alloys Comp.*, **221** (1995) 86.
- [3] S. Okada, T. Atoda and I. Higashi, *J. Solid State Chem.*, **68** (1987) 61.
- [4] S. Okada, K. Hamano, T. Lundström and I. Higashi, in D. Emin et al. (eds.), *Boron-rich Solids*, AIP Conf. Proc. No. 231, American Institute of Physics, New York, 1991, p. 456.
- [5] M.V. Chepiga, V.P. Krivutskii and Yu.B. Kuz'ma, *Izv. Akad. Nauk SSSR Neorg. Mater.*, **8** (1972) 1059.
- [6] Yu. B. Kuz'ma and P.K. Starodub, *Izv. Akad. Nauk SSSR Neorg. Mater.*, **9** (1973) 376.
- [7] D. Elwell and H.J. Scheel, *Crystal Growth from High-Temperature Solutions*, Academic Press, London, 1975.
- [8] T. Lundström, *J. Less-Common Met.*, **100** (1984) 215.
- [9] R.D. Deslattes and A. Henins, *Phys. Rev. Lett.*, **31** (1973) 972.
- [10] B.I. Noläng, personal communication, Institute of Chemistry, Uppsala, 1989.
- [11] TEXSAN: *Single Crystal Structure Analysis Software*, Version 5.0, Molecular Structure Corporation, The Woodlands, TX, 1989.
- [12] J.-O. Lundgren (ed.), *Crystallographic computer programs*, Institute of Chemistry, Uppsala University, 1982.
- [13] H. Bolmgren and T. Lundström, *J. Less-Common Met.*, **159** (1990) L25.